

Ruthenium(II) hydrido complexes of quadridentate crown thioethers, *trans*-RuH(Cl)(*syn*-L) (L = Me₄[14]aneS₄, Me₆[15]aneS₄, Me₈[16]aneS₄) and {Ru₂H(μ-H)Cl(*syn*-Me₄[14]aneS₄)₂}Cl containing a linear Ru–H–Ru bond. Novel characteristics of *syn*-crown thioethers affecting discrimination of axial ligands and geometry of the unsupported Ru–H–Ru linkage

Toshikatsu Yoshida^a, Tomohiro Adachi^a, Tatsuo Ueda^a, Fumitaka Goto^b, Katsumi Baba^a, Toshihiro Tanaka^a

^a Department of Chemistry, Faculty of Integrated Arts and Sciences, University of Osaka Prefecture, Sakai, Osaka 593 (Japan)

^b Industrial Research Divisions, Otsuka Pharmaceutical Co. Ltd., Tokushima 777-01 (Japan)

(Received November 17, 1993; in revised form December 22, 1993)

Abstract

A series of ruthenium(II) hydrido complexes containing crown thioethers, *trans*-RuH(Cl)(*syn*-L) (4, L = Me₄[14]aneS₄; 5, L = Me₆[15]aneS₄; 6, L = Me₈[16]aneS₄), were prepared in good yields by treating the corresponding dichlorides *cis*-RuCl₂L (1, L = Me₄[14]aneS₄; 2, L = Me₆[15]aneS₄; 3, L = Me₈[16]aneS₄) with NaBH₄ in MeOH for 4 and in EtOH for 5 and 6. The structures of 4 and 5 were elucidated by an X-ray diffraction study: 4, orthorhombic, space group *Pna*2₁ (No. 33), *a* = 14.683(13), *b* = 12.605(2), *c* = 10.284(7) Å, *Z* = 4, *R*(*R_w*) = 0.030(0.033) for 2303 reflections ($|F_o| \geq 6\sigma(F_o)$); 5, orthorhombic, *Pbca* (No. 61), *a* = 14.976(3), *b* = 13.877(3), *c* = 21.079(27) Å, *Z* = 8, *R*(*R_w*) = 0.043(0.051) for 3011 reflections ($|F_o| \geq 5\sigma(F_o)$). The hydrido ligand in 4 and the chloro anion in 5 coordinate specifically at the congested axial site surrounded by the ring carbon atoms of the *syn*-crown thioethers. By contrast, the stereochemically different axial sites of the Ru(*syn*-Me₈[16]aneS₄) moiety in 6 failed to discriminate between the two axial ligands and 6 exists as a mixture of two geometrical isomers. A similar reaction of 1 with NaBH₄ in EtOH gave an unsupported bridging hydride {Ru₂H(μ-H)Cl(*syn*-Me₄[14]aneS₄)₂}Cl (7) as the major product together with 4. Compound 7 crystallizes in the trigonal, space group, *R3c* (No. 167), with *a* = 18.615(6), *c* = 64.937(13) Å, *Z* = 18. Least-squares refinement of 1975 reflections ($|F_o| \geq 6\sigma(F_o)$) gave a final *R*(*R_w*) = 0.055(0.063). The cation of 7 possesses crystallographically *C*₂ symmetry with a face to face disposition of the RuH(*syn*-Me₄[14]aneS₄) and RuCl(*syn*-Me₄[14]aneS₄) moieties which are connected through a μ-hydride. The μ-hydride is completely surrounded by the lone pair orbitals of eight S atoms of the two moieties in a staggered conformation. The rotational barrier of the two moieties about the Ru–H–Ru bond assessed by extended Hückel MO calculations on the model compound {Ru₂H(μ-H)Cl(*syn*-(SH₂)₄)₂}⁺ of *C*_{4v} symmetry is 0.82 eV. The calculations also indicated that the linear Ru–H–Ru geometry is more stable than the bent one; the elevation in total energy on bending the Ru–H–Ru linkage by 20° from linearity is 0.78 eV. Structural flexibility of *syn*-Me₄[14]aneS₄ was proved from the molecular structure of 7 where a bulky chloro ligand is accommodated at the congested axial site of the Ru(*syn*-Me₄[14]aneS₄) moiety. In sharp contrast to the facile displacement of all PPh₃ ligands in RuCl₂(PPh₃)₃ by the crown thioethers employed here to give 1–3, an attempt to prepare 4 by treating RuHCl(PPh₃)₃ with Me₄[14]aneS₄ failed and RuH(Cl₂)(PPh₃)₂Me₄[14]aneS₄ (9) was obtained. The chloride and one of two PPh₃ ligands of 9 readily dissociate in MeOH affording *cis*-(RuH(PPh₃)₂Me₄[14]aneS₄)Cl₂ (10).

Key words: Ruthenium; Ruthenium(II) hydrides; Crown thioethers; Linear Ru–H–Ru bond; Extended Hückel calculations

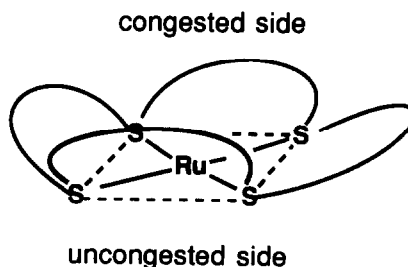
1. Introduction

In tetragonal complexes of quadridentate macrocycles, the coordination of axial ligands has been shown to be severely affected by steric encumbrance. A typical example is the so-called distal-side steric effect

Correspondence to: Dr. T. Yoshida.

upon the relative binding affinity of CO versus O₂ to Fe^{II} porphyrin complexes [1]. A similar steric control of CO and O₂ coordinations is known for lacunar tetraazacyclohexadecatetraene complexes, Fe((*m*-xyl-yl)(RNEthi)₂[16]tetraeneN₄) Cl (R = H, Me; Eth = ethylidene) and related Co^{II} complexes, respectively [2,3]. The difference in stereochemical congestion at the axial sites in {Co(rac-(N)-Me₆[16]dieneN₄)XY}ⁿ⁺ (X = NO₂, Y = Cl, *n* = 1; X = H₂O, Y = CH₃, *n* = 2) has also been shown to affect the reactivity towards substitution of axial ligands [4]. Saturated quadridentate crown thioethers in a planar coordination can adopt several conformations, *syn*, *anti*, and so on (Fig. 1). In the *syn* conformer the two axial sites are in stereochemically very different environments as shown below; the site surrounded by the ring carbon atoms is congested, while the opposite site is uncongested. Therefore, two ligands possessing different steric demands are expected to be discriminated by these two axial sites on coordination. Indeed, we have recently confirmed this type of novel recognition for the two

π -acidic functionalities of PhNCO in *trans*-Mo(η^2 -O,



C-PhNCO)(η^2 -C,N-PhNCO)(*syn*-Me₈[16]aneS₄) where the η^2 -C,N-PhNCO, more sterically demanding than η^2 -O,C-PhNCO, occupies the uncongested axial site stereospecifically [5]. In addition, the room to accommodate an axial ligand at the congested site may be controlled by the ring size of the macrocycles. To verify this type of recognition further for the anionic ligands, H⁻ and Cl⁻, and for the ring size effect, we have prepared a series of mononuclear Ru^{II} hydrido chloro complexes containing 14–16 membered crown

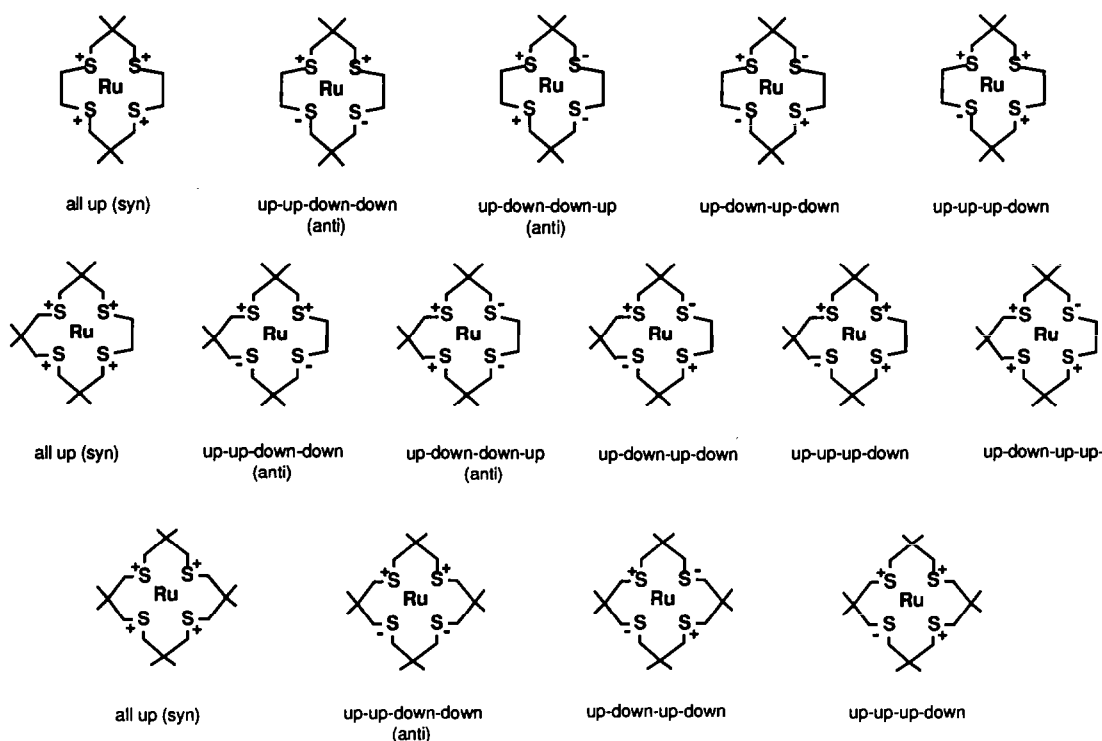


Fig. 1. Conformations of 14–16-membered quadridentate crown thioethers in planar coordination. + and - indicate the direction of the free pair orbitals on the S atoms with respect to the equatorial 4S plane.

thioethers in *syn*-conformation, *trans*-RuH(Cl)(*syn*-L) (4, L = Me₄[14]aneS₄; 5, L = Me₆[15]aneS₄; 6, L = Me₈[16]aneS₄) (Me₄[14]aneS₄ = 6,6,13,13-tetramethyl-1,4,8,11-tetrathiacyclotetradecane, Me₆[15]aneS₄ = 6,6,10,10,14,14-hexamethyl-1,4,8,12-tetrathiacyclopentadecane, Me₈[16]aneS₄ = 3,3,7,7,11,11,15,15-octamethyl-1,5,9,13-tetrathiacyclohexadecane). We also report the preparation and X-ray structure of a novel μ -hydrido complex {Ru₂H(μ -H)Cl(*syn*-Me₄[14]aneS₄)₂}Cl (7) bearing neither supporting bridging ligands nor metal-metal bonding. The X-ray structural studies of 4 and 5 showed that the congested axial sites in the Ru(*syn*-Me₄[14]aneS₄) and Ru(*syn*-Me₆[15]aneS₄) fragments have the spatial volume suitable to accommodate the hydrido and chloro ligands, respectively. In contrast, the corresponding cavity of the Ru(*syn*-Me₈[16]aneS₄) moiety in 6 proved to be too large to recognize these two anionic ligands. Unexpectedly from the molecular structure of 4, the chloro ligand of the RuCl(*syn*-Me₄[14]aneS₄) fragment in 7 was confirmed to occupy the congested axial site. Therefore, we discuss the structural flexibility of *syn*-Me₄[14]aneS₄ which is capable of adjusting the hole size surrounded by the ring carbon atoms depending upon the steric requirement of the anion to be accommodated.

Most M-H-M bonds of transition metals so far reported are supported by additional bridging ligands and/or distinct metal-metal bonding, whereas unsupported μ_2 -hydrido complexes are still a rarity. As far as we know, [M₂(μ -H)(CO)₁₀]⁻ (M = Cr, Mo, W) [6], [W₂(μ -H)(CO)₉NO] [7], (η^5 -C₅H₅)₂Nb(μ -H)M(η^5 -C₅H₅)(CO)₃ (M = Nb, V) [8], and ((η^5 -C₅H₅)₂WH(μ -

H)PtPh(PEt₃)₂]⁺ [9] are the only hydrido complexes characterized so far by X-ray and neutron diffraction studies. The M-H-M three-center two-electron (3c-2e) bond of transition metals is known to be inherently bent [6,10,11]. The crystallographic C₂ symmetry of 7 and the location of the bridging hydride in the cage constructed by interlocking the eight free lone pair orbitals on sulfur atoms of the RuH(*syn*-Me₄[14]aneS₄) and RuCl(*syn*-Me₄[14]aneS₄) moieties, which are in a face to face disposition with a staggered conformation, should strongly support the linear Ru-H-Ru geometry. The Ru-H-Ru linkage in this rather unusual environment might be destabilized on bending since such deformation would increase the electrostatic repulsions between the free lone pair electrons of the two moieties. Therefore, the effect of these free lone pair orbitals of the sulfur atoms upon the geometry of the Ru-H-Ru 3c-2e bond in 7 was studied theoretically by extended Hückel MO calculations. Some of the preliminary aspects have been published previously [12,13].

2. Results and discussion

2.1. Preparation of ruthenium(II) hydrido complexes containing crown thioethers

The starting dichlorides *cis*-RuCl₂L (1, L = Me₄[14]aneS₄ [14]; 2, L = Me₆[15]aneS₄; 3, L = Me₈[16]aneS₄) employed for the preparation of the hydrides 4-6 were obtained by heating RuCl₂(PPh₃)₃ with the corresponding crown thioethers in toluene (80°C) in

TABLE 1. ¹H NMR spectral data of *cis*-RuCl₂L (1-3) ^a

L	CH ₃	SCH ₂ CMe ₂	SCH ₂ CH ₂ S
Me ₄ [14]aneS ₄ (1)	1.09 (s, 3H)	2.41 (d, 1H); 2.67 (d, 1H)	2.38 (m, 1H); 2.94 (m, 2H)
	1.13 (s, 3H)	<i>J</i> = 10.7 <i>J</i> = 15.0	3.31 (m, 1H)
Me ₆ [15]aneS ₄ (2)	1.09 (s, 6H)	2.97 (d, 1H); 3.52 (d, 1H)	2.28 (m, 1H); 2.87 (m, 2H) 2.95 (m, 1H)
	1.16 (s, 3H)	<i>J</i> = 15.0 <i>J</i> = 10.7	
	1.19 (s, 3H)	2.05 (d, 1H); 2.07 (d, 1H)	
	1.24 (s, 3H)	<i>J</i> = 11.6 <i>J</i> = 11.9	
	1.25 (s, 3H)	2.40 (d, 1H); 2.43 (d, 1H)	
		<i>J</i> = 11.0 <i>J</i> = 14.0	
		2.52 (d, 1H); 2.55 (d, 1H)	
		<i>J</i> = 8.1 <i>J</i> = 8.1	
		2.62 (d, 1H); 2.85 (d, 1H)	
		<i>J</i> = 13.8 <i>J</i> = 14.0	
Me ₈ [16]aneS ₄ (3)	1.17 (s, 3H)	3.21 (d, 1H); 3.37 (d, 1H)	
	1.21 (s, 3H)	<i>J</i> = 13.8 <i>J</i> = 11.6	
		3.96 (d, 1H); 4.07 (d, 1H)	
		<i>J</i> = 11.0 <i>J</i> = 11.9	
		2.07 (d, 1H); 2.67 (d, 1H)	
	<i>J</i> = 11.6 <i>J</i> = 12.8		
	3.03 (d, 1H); 3.70 (d, 1H)		
	<i>J</i> = 12.8 <i>J</i> = 11.6		

^a Measured in CDCl₃, *J* in Hz.

quantitative yields. The complete substitution of all the PPh₃ ligands by the 14–16 membered crown thioethers contrasts sharply with a similar reaction of [9]aneS₃ and [12]aneS₄ which afforded RuCl₂(PPh₃)([9]aneS₃) and {RuCl(PPh₃)([12]aneS₄)}⁺, respectively [15]. *cis*-Stereochemistry of **1**, **2** and **3** was readily deducible from the IR spectra showing two $\nu(\text{Ru}-\text{Cl})$ bands (245 and 260, 256 and 261, and 258 and 270 cm⁻¹, respectively). Consistently, the ¹H NMR spectra of **1** and **2** show four and twelve signals due to the CH₂ protons of RuSCH₂CMe₂CH₂S rings, respectively (Table 1). Similarly, the observation of the four corresponding signals for **3** is compatible with a *cis* geometry. The *cis* geometry of RuCl₂([14]aneS₄) has been confirmed by an X-ray structural study [16].

Treatment of **1** with an excess of NaBH₄ in EtOH at ambient temperature gave *trans*-RuH(Cl)(*syn*-Me₄-[14]aneS₄) (**4**) as yellow crystals together with brown crystals of a μ -hydrido complex {Ru₂H(μ -H)Cl(*syn*-Me₄[14]aneS₄)₂}Cl (**7**) in 16 and 54% yields, respec-

tively. The ratio of the two hydrides may be dependent on the solvents employed and **4** was obtained as the sole product (81%) when the reaction was carried out in MeOH. A similar reaction of **2** and **3** with an equimolar amount of NaBH₄ in EtOH afforded the corresponding hydrides **5** (49%) and **6** (74%), respectively. In both cases, the Me₆[15]aneS₄ and Me₈[16]aneS₄ analogues of **7** were not detected at all, indicating that the ring size of the macrocycles is crucial for the formation of the dinuclear μ -hydrido complex. The ring size also affects the reactivity of the chloro ligand in **4**–**6** towards NaBH₄. Thus, **5** and **6** react further with excess NaBH₄ at room temperature to give *trans*-RuH(η^1 -BH₄)L (L = *syn*-Me₆[15]aneS₄, *anti*-Me₈[16]aneS₄) [17], while **4** and **7** failed to react at least under similar conditions. All the hydrido complexes thus obtained are extremely unstable in air and soluble in polar solvents. The Me₄[14]aneS₄ complex **4** differs from the 15- and 16-membered analogues **5** and **6** in its solubility in aromatic hydrocarbons; the former crystals

TABLE 2. Spectral data of Ru^{II} hydrido complexes

	IR (cm ⁻¹) ^a $\nu(\text{Ru}-\text{H})$	¹ H NMR (δ) ^b			
		RuH	CH ₃	SCH ₂ CMe ₂	SCH ₂ CH ₂ S
<i>trans</i> -RuH(Cl)Me ₄ [14]aneS ₄ ^c (4)	1958	-23.1 (s, 1H)	1.12 (s, 6H) 1.24 (s, 6H)	2.27 (d, 4H); 3.18 (d, 4H) J = 10.5 J = 10.5	2.39 (m, 4H) 3.07 (m, 4H)
<i>trans</i> -RuH(Cl)Me ₆ [15]aneS ₄ ^d (5)	1908	-20.9 (s, 1H)	0.70 (s, 3H) 0.83 (s, 6H) 1.03 (s, 6H) 1.21 (s, 3H)	1.95 (d, 2H); 2.13 (d, 4H) J = 11.0 J = 11.0 2.89 (d, 2H); 3.88 (d, 2H) J = 11.0 J = 11.0 3.94 (d, 2H) J = 11.0	2.29 (m, 2H) 2.77 (m, 2H)
<i>trans</i> -RuH(Cl)Me ₈ [16]aneS ₄ ^d (6)	1860	-21.6 (s, 1H)	1.08 (s, 12H)	2.32 (d, 8H); 3.09 (d, 8H)	
	1904	-21.7 (s, 1H)	1.10 (s, 12H) 1.24 (s, 12H)	2.27 (d, 8H); 3.18 (d, 8H) J = 11.0 J = 11.0	
[Ru ₂ H(μ -H)Cl(Me ₄ [14]aneS ₄) ₂] ^{+c,e} (7)	1820	-20.8 (d, 1H) J = 13.9 -33.3 (s, 1H) J = 13.9	1.03 (s, 6H) 1.04 (s, 1H) 1.07 (s, 6H) 1.10 (s, 6H)	1.91 (d, 4H); 2.44 (d, 4H) J = 9.9 J = 9.9 3.09 (d, 4H); 3.78 (d, 4H) J = 10.9 J = 10.9	~ 2.3 (m, 4H) ~ 2.28 (m, 4H) ~ 3.0 (m, 4H)
{RuHMe ₄ [14]aneS ₄ } ^{+f} (8)	1983	-26.0 (s, 1H)	1.16 (s, 6H) 1.18 (s, 6H)	2.24 (d, 4H); 3.37 (d, 4H) J = 10.9 J = 10.9	2.69 (m, 4H) 3.12 (m, 4H)
RuH(Cl)(PPh ₃) ₂ Me ₄ [14]aneS ₄ · dme ^{d,g} (9)	2030	-18.8 (t, 1H) J(PH) = 24.3	0.50 (s, 6H) 0.73 (s, 6H)	1.89 (d, 2H); 2.61 (d, 2H) J = 13.9 J = 13.9 2.73 (d, 2H); 3.18 (d, 2H) J = 13.9 J = 13.9	2.4–2.6 (m, 4H)
{RuH(PPh ₃)Me ₄ [14]aneS ₄ } ^{+f} (10)	1875	-10.3 (d, 1H) J(PH) = 22.9	0.58 (s, 3H)	1.88 (d, 1H); 2.39 (d, 1H)	1.73 (m, 1H)
			1.03 (s, 3H)	J = 12.7 J = 11.7	2.46 (m, 1H)
			1.21 (s, 3H)	2.59 (d, 1H); 2.64 (d, 1H)	2.96 (m, 1H)
			1.26 (s, 3H)	J = 13.7 J = 12.7 2.80 (d, 1H); 2.97 (d, 1H) J = 13.7 J = 11.7 3.34 (d, 1H); 3.56 (d, 1H) J = 12.7 J = 12.7	2.98 (m, 1H) 3.10 (m, 1H) 3.20 (m, 1H) 3.32 (m, 1H) 3.56 (m, 1H)

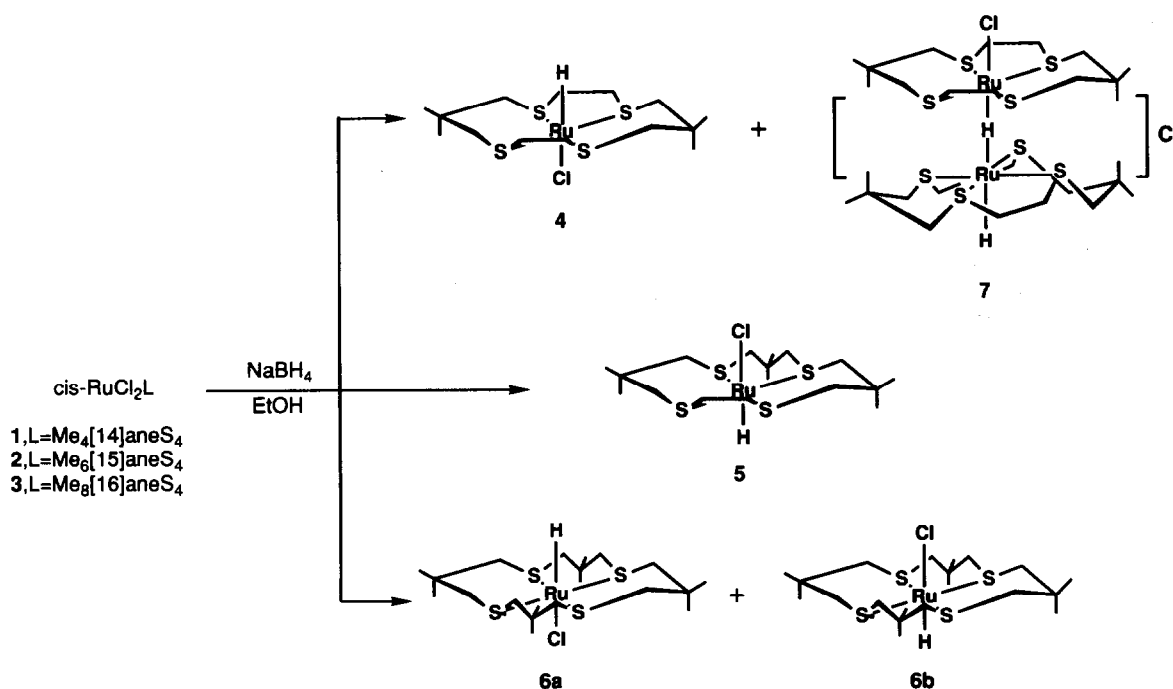
^a Nujol mull. ^b J in Hz. ^c In CD₂Cl₂. ^d In benzene-d₆. ^e The ratio of two geometrical isomers exhibiting the hydrido signals at δ -21.6 and -21.7 is 2:3. ^f In acetone-d₆. ^g Signals due to dme appear at δ 3.12 (s, 6H, Me) and 3.31 (s, 4H, CH₂).

are practically insoluble, while the latter two are readily soluble. The difference in solubility between **4** and **5** is associated with their molecular packings in crystals rather than the ionic character of the Ru–Cl bonds (*vide infra*).

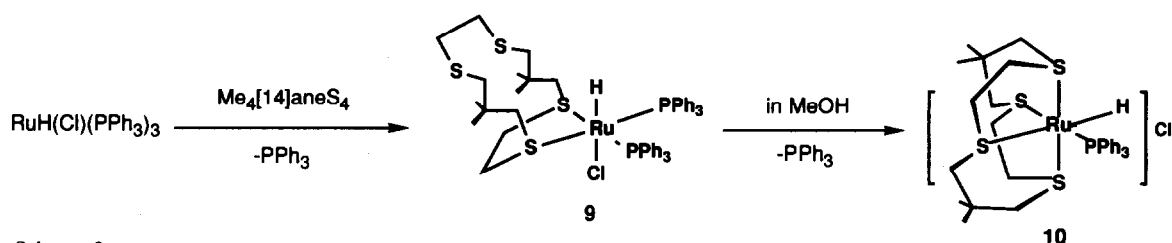
In sharp contrast to the *cis* geometry of the parent dichlorides where the crown thioethers adopt a folded form, the ¹H NMR spectra of **4**–**6** (Table 2) indicate that the macrocycles girdle the equatorial positions. This type of planar coordination gives rise to five, six, and four possible conformers for **4**, **5** and **6**, respectively (Fig. 1). The observation of two signals for each Me and CH₂ group of the RuSCH₂CMe₂CH₂S rings of **4** is only consistent with a *syn* conformation of Me₄[14]aneS₄ with mutually *trans* hydrido and chloro ligands at the axial sites. In contrast, the ¹H NMR spectrum of **5** exhibiting four Me and six CH₂ proton signals due to the fused three RuSCH₂CMe₂CH₂S rings fails to discriminate between the two possible conformers, *syn* and one of two *anti* forms (up-down-down-up). In the latter, the middle and two outer six-membered chelate rings assume chair and twist forms, respectively. A *syn* conformation of Me₆[15]aneS₄ was confirmed by the X-ray structure of **5** (*vide infra*). Due to the axial asymmetry expected for the *syn*-conformer, two geometrical isomers are possible for **4** and **5**. However, the ¹H NMR and IR spectra indicate the presence of only one isomer both in solution and in the solid state. The relative position of

hydrido and chloro ligands with respect to the ring carbon atoms of the *syn*-macrocycles was determined unequivocally by the X-ray structural analyses of **4** and **5** (*vide infra*). The Me₈[16]aneS₄ ligand in **6** also assumes a *syn* conformation. However, the spectral data indicate the existence of two possible geometrical isomers **6a** and **6b** shown in Scheme 1 in a ratio of 2:3.

An ionic character of the binuclear μ -hydrido complex {Ru₂H(μ -H)Cl(*syn*-Me₄[14]aneS₄)₂}Cl (**7**) was shown by the metathesis reaction with NaBPh₄ in MeOH affording the corresponding salt. The ¹H NMR spectrum shows the presence of two inequivalent hydrido ligands and two chemically different Me₄[14]aneS₄ macrocycles both adopting *syn* conformation (Table 2). The observation of a very strong ν (Ru–H) band due to the terminal hydride at 1820 cm⁻¹, which is considerably lower in frequency than that (1958 cm⁻¹) of **4**, indicates the presence of a μ -hydride of strong *trans* influence at the opposite axial site rather than a μ -Cl ligand. Consistent with this, a strong coupling between the two hydrido ligands are observed with ²J(HH) of 13.9 Hz. The single crystal X-ray diffraction study of **7** confirmed unequivocally the structural features proposed on the basis of the spectral data (*vide infra*). A plausible step for the formation of **7** may be a nucleophilic attack of the hydrido ligand of **4** on a five-coordinated [RuH(*syn*-Me₄[14]aneS₄)]⁺ species formed through dissociation of the chloro ligand. A related nucleophilic substitution of the Cl ligand in *cis*-



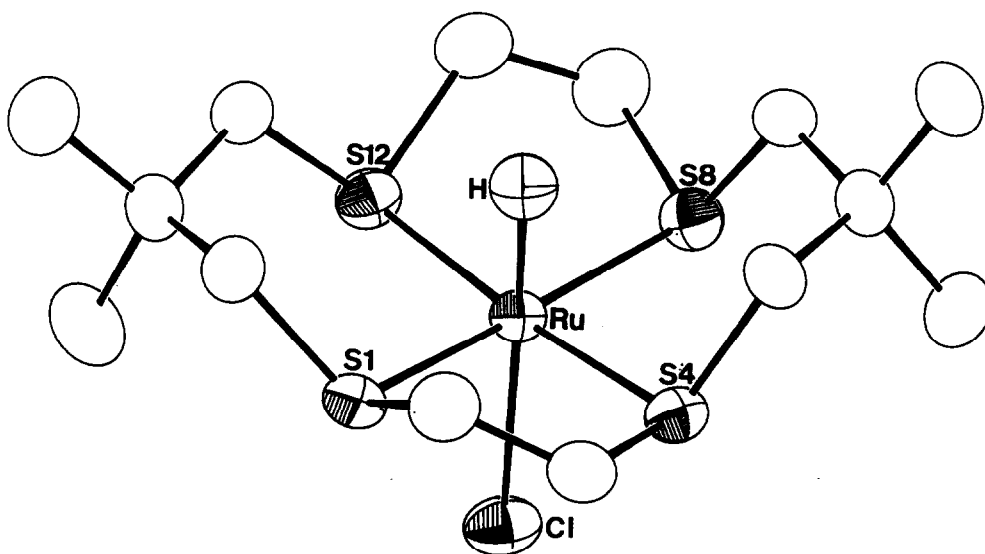
Scheme 1.



Scheme 2.

PtH(Cl)L (L = (^tBu)₂PCH₂CH₂P(^tBu)₂) by the hydrido ligand of the corresponding dihydride *cis*-PtH₂L has been proposed for the formation of [Pt₂(H)₂(μ-H)-L₂]⁺ [18]. The facile dissociation of the coordinated chloro ligand in 4 is manifested by the precipitation of {RuH(*syn*-Me₄[14]aneS₄)BPh₄} (8) on addition of NaBPh₄ to the EtOH solution. A tetragonal pyramidal structure with four S atoms of *syn*-Me₄[14]aneS₄ in the basal plane and the hydrido ligand at the apical site was deduced from the spectral data (Table 2). An alternative octahedral structure with the coordinated solvent at the vacant axial site was readily excluded from the elemental analysis and absence of ν(C=O) band in the IR spectrum of the sample recrystallized from acetone. However, an attempt to prepare 7 by treating 4 and 8 in acetone failed, both starting materials being recovered unchanged. Rationales for the ring size effect of crown thioethers and the solvent effect observed for the formation of the cationic μ-hydrido complex 7, as well as its formation mechanism, still remain to be elucidated.

In view of the facile and complete substitution of all PPh₃ ligands in RuCl₂(PPh₃)₃ by the 14–16-membered quadridentate crown thioethers, the corresponding reactions of RuH(Cl)(PPh₃)₃ may provide an alternative route to 4–6. Indeed, one of the coordinated PPh₃ in RuH(Cl)(PPh₃)₃ was readily displaced by Me₄[14]aneS₄ at room temperature in dimethoxyethane affording RuH(Cl)(PPh₃)₂(Me₄[14]aneS₄) (9) in a reasonable yield. The ¹H NMR spectrum shows a hydrido signal as a triplet with *J*(PH) = 24.3 Hz which is in the range of magnitude of *cis* coupling constants between a hydrido and phosphine phosphorus atom in Ru^{II} complexes [18]. The observation of two methyl and four CH₂ proton signals due to the SCH₂CMe₂CH₂S groups suggests that the molecule possesses C_s symmetry. Thus, the hydrido ligand is *cis* to the two mutually *cis* PPh₃ ligands and Me₄[14]aneS₄ coordinates as a bidentate ligand at the equatorial sites forming a RuS-CH₂CH₂S ring rather than a six-membered chelation. The plausible structure deduced from the spectral data is shown in Scheme 2. An attempt to prepare 4 by

Fig. 2. Molecular structure of *trans*-RuH(Cl)(*syn*-Me₄[14]aneS₄) (4). Thermal ellipsoids are drawn at 50% probability.

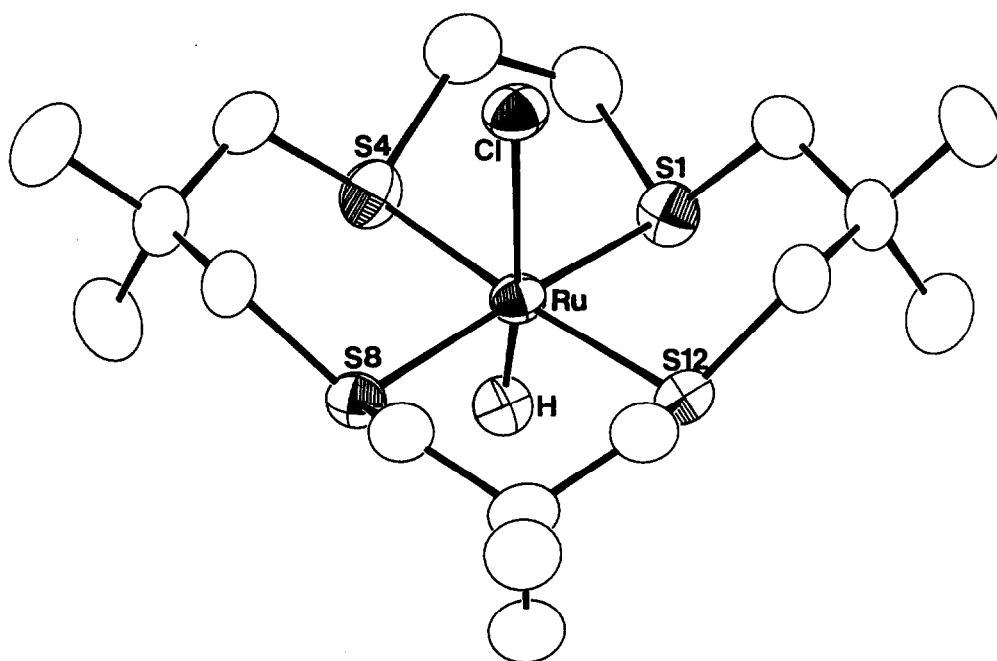


Fig. 3. Molecular structure of *trans*-RuH(Cl)(*syn*-Me₆[15]aneS₄) (5). Thermal ellipsoids are drawn at 50% probability.

heating **9** in dme (dimethoxyethane) or toluene (80°C) failed, **9** being recovered unchanged. This is in sharp contrast to the complete displacement of PPh₃ ligands in RuCl₂(PPh₃)₃ by the crown thioethers under similar

conditions. On dissolving **9** in MeOH at room temperature, however, both the chloro anion and one of two PPh₃ ligands dissociated readily affording *cis*-{RuH(PPh₃)(Me₄[14]aneS₄)}Cl (**10**), which was isolated as

TABLE 3. Selected bond distances (Å) and angles (°) of *trans*-RuH(Cl)(*syn*-L) (4, L = Me₄[14]aneS₄; 5, L = Me₆[15]aneS₄)

4				5			
Ru–H	1.68(8)	H–Ru–Cl	174.5(23)	Ru–H	1.534(7)	H–Ru–Cl	173.6(24)
Ru–Cl	2.559(2)	H–Ru–S(1)	85.3(22)	Ru–Cl	2.618(2)	H–Ru–S(1)	86.6(23)
Ru–S(1)	2.280(2)	H–Ru–S(4)	85.1(22)	Ru–S(1)	2.295(3)	H–Ru–S(4)	83.1(25)
Ru–S(4)	2.307(2)	H–Ru–S(8)	89.5(22)	Ru–S(4)	2.308(2)	H–Ru–S(8)	85.3(23)
Ru–S(8)	2.308(2)	H–Ru–S(11)	90.0(22)	Ru–S(8)	2.298(3)	H–Ru–S(12)	94.9(25)
Ru–S(11)	2.292(2)	Cl–Ru–S(1)	90.0(1)	Ru–S(12)	2.316(2)	Cl–Ru–S(1)	97.2(1)
S(1)–C(2)	1.821(5)	S(1)–Ru–S(4)	87.5(1)	S(1)–C(2)	1.838(8)	S(1)–Ru–S(4)	84.8(1)
S(1)–C(14)	1.822(6)	S(1)–Ru–S(8)	173.9(1)	S(1)–C(15)	1.808(7)	S(1)–Ru–S(8)	171.4(1)
S(4)–C(3)	1.837(5)	S(1)–Ru–S(11)	94.9(1)	S(4)–C(3)	1.838(8)	S(1)–Ru–S(12)	87.8(1)
S(4)–C(5)	1.821(5)	S(4)–Ru–S(8)	89.1(1)	S(4)–C(5)	1.817(6)	S(4)–Ru–S(8)	91.4(1)
S(8)–C(7)	1.826(5)	S(4)–Ru–S(11)	174.4(1)	S(8)–C(7)	1.841(6)	S(4)–Ru–S(12)	172.5(1)
S(8)–C(9)	1.819(7)	S(8)–Ru–S(11)	88.1(1)	S(8)–C(9)	1.825(6)	S(8)–Ru–S(12)	95.6(1)
S(11)–C(10)	1.839(7)			S(12)–C(11)	1.820(6)		
S(11)–C(12)	1.825(5)			S(12)–C(13)	1.818(6)		
Intramolecular non-bonded contacts							
H···H(C(2))	2.60			Cl···H(C(3))	2.93		
H···H(C(5))	2.34			Cl···H(C(5))	2.77		
H···H(C(7))	2.40			Cl···H(C(7))	2.84		
H···H(C(10))	2.76			Cl···H(C(9))	3.15		
H···H(C(12))	2.76			Cl···H(C(11))	3.22		
H···H(C(14))	2.65			Cl···H(C(15))	2.83		

the BPh₄⁻ salt. The ¹H NMR spectrum suggests a *cis* disposition of the hydrido and PPh₃ ligands with a folded tetradentate coordination of Me₄[14]aneS₄. An attempt to prepare RuH(Cl)(PPh₃)₂(Me₈[16]aneS₄) by treating RuCl(PPh₃)₃ with the corresponding crown thioether under similar reaction conditions employed for the preparation of **9** failed. Both starting materials were recovered unchanged.

2.2. Crystal and molecular structures of *trans*-RuH(Cl) (*syn*-L) (**4**, L = Me₄[14]aneS₄; **5**, L = Me₆[15]aneS₄) and {Ru₂H(μ-H)Cl(*syn*-Me₄[14]aneS₄)₂}Cl (**7**)

Figures 2 and 3 show the molecular structures of **4** and **5** as determined by an X-ray diffraction study with a numbering scheme, respectively. Bond lengths and angles are compiled in Table 3. The geometry about the Ru atom of both hydrides is slightly distorted octahedral with the four S atoms of the *syn*-crown thioethers in the equatorial plane and the hydrido and chloro ligands at the axial positions. The average Ru–S distance (2.297(2) Å) of **4** is comparable with that (2.304(3) Å) of **5**. These bonds are significantly shorter than the corresponding separations *trans* to the S atom found in *cis*-RuCl₂[14]aneS₄ (2.336(1) Å) [16], [Ru([12]aneS₃)₂]²⁺ (2.3728(4) Å) [20] and [(Ru[9]aneS₃)₂]²⁺ (2.339(1) Å [21], 2.332(1) Å [22]). The contraction is probably due to the small cavity of *syn*-Me₄[14]aneS₄ and *syn*-Me₆[15]aneS₄ compared to the ionic radius of the Ru^{II} ion. In fact, the Ru atom in **4** and **5** is forced to deviate from the 4S plane defined by the four S atoms with the pyramidal distortion (average *trans* S–Ru–S angle 174.1(1)° and 172.0(1)°, respectively). It is worth noting that the two hydrides differ in the location of the hydrido ligand at the axial sites of very different stereochemical congestion. The Ru atoms in **4** and **5** are also displaced from the 4S plane in different directions; in the latter towards the congested axial site surrounded by the ring C atoms by 0.099(1) Å, while in the former towards the opposite uncluttered side by 0.101(1) Å. The deviation of the four S atoms from the least-squares 4S plane is ±0.001(1) Å for **4** and ±0.060(2) Å for **5**. The rationale for the differences is discussed later.

The interesting solubility difference in aromatic hydrocarbons between **4** and **5** may be accounted for by their molecular packings in crystals (Fig. 4). The crystal structure of the former is acentric and the *trans*-H–Ru–Cl dipoles align in the same direction along the *c*-axis, while that of the latter is centric and the dipoles are totally cancelled out. Thus, the insolubility of the former and the high solubility of the latter in toluene are ascribed to the presence and absence of an intrinsic polarization in their crystals, respectively. In contrast, the short Ru–Cl distance (2.559(2) Å) of **4** com-

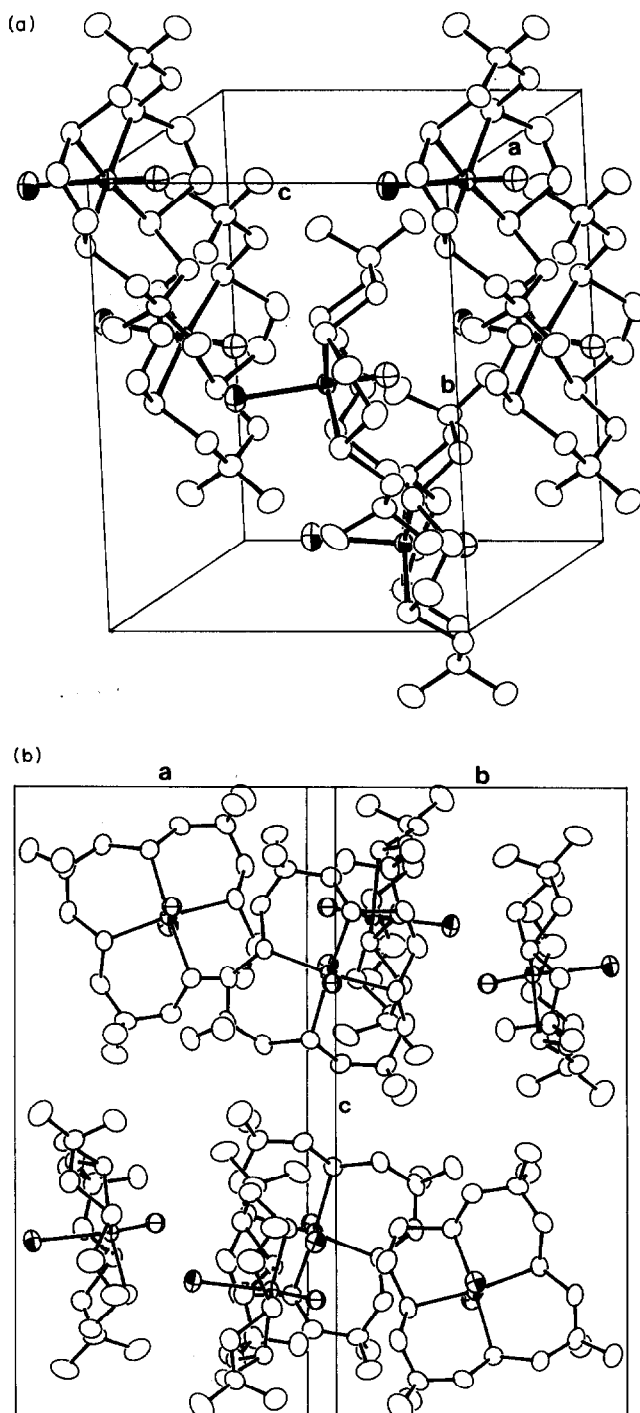


Fig. 4. Crystal packings of *trans*-RuH(Cl)(*syn*-Me₄[14]aneS₄) (**4**) (a) and *trans*-RuH(Cl)(*syn*-Me₆[15]aneS₄) (**5**) (b).

pared to that (2.618(2) Å) of **5** indicates that the polarization of the Ru–Cl bond in the former is less than that of the latter.

The molecular structure of **7** is depicted in Fig. 5 with the atom numbering scheme. The important bond

lengths and angles are shown in Table 4. As deduced from the spectral data, the two fragments RuH(*syn*-Me₄[14]aneS₄) and RuCl(*syn*-Me₄[14]aneS₄) with a face to face disposition are connected together through the bridging hydride (H_b). Both the terminal hydride (H_t) and Cl ligands in these fragments are located at the congested axial sites. Note that the axial site occupied by the Cl ligand differs from that found for **4**. The Cl, Ru1 and Ru2 atoms are exactly colinear. The least-squares plane defined by the four S atoms of the RuCl(*syn*-Me₄[14]aneS₄) moiety is also strictly parallel with the corresponding plane of the other fragment. The deviations of the S atoms from the 4S plane in the former and the latter are ±0.019(5) and ±0.040(4) Å, respectively. The equatorial 4S planes of the two fragments are mutually staggered with the torsion angle S1(1)–Ru1–Ru2–S2(4) of 54.3(1)° (Fig. 5(b)). Thus, the molecule possesses crystallographic C₂ symmetry. The Ru1–H_b, Ru2–H_b, and Ru2–H_t lengths are 1.82(15), 1.60(15), and 1.69(13) Å, respectively. The average Ru1–S and Ru2–S distances (2.292(3) and 2.299(3) Å, respectively) are very similar to the corresponding mean separations found in **4** and **5** (*vide supra*).

2.3. Ring size effect of the crown thioethers upon the discrimination of axial ligands and the structural flexibility of *syn*-Me₄[14]aneS₄

The most conspicuous difference in the structures between **4** and **5** is the position of the hydrido ligand (and chloro anion) at the stereochemically different axial sites. Thus, the hydrido ligand in the former is located specifically at the congested site, while in the latter at the uncongested site. The Ru–H distances of **4** and **5** are 1.68(8) and 1.534(7) Å, respectively. The hydrido ligand in **4** is in van der Waals contact with the axial hydrogen atoms of the ring C(5) and C(7) atoms

with non-bonded distances of 2.34 and 2.40 Å, respectively (Table 3). This probably indicates that the cavity created by the ring C atoms of the Ru(*syn*-Me₄[14]aneS₄) moiety is suitable in size to accommodate the hydrido ligand, but is too small for the Cl anion. On increasing the ring size of crown thioethers from the 14- to the 15-membered ring, the cavity around the congested axial site is dilated enough to admit the more bulky chloro ligand. Then a question arises concerning the origin for the discrimination of the two anionic ligands. The stereospecific coordination of the chloro ligand rather than the hydride at the congested axial site in **5** may be explained by attractive van der Waals interactions with the axial CH₂ hydrogen atoms of *syn*-Me₆[15]aneS₄, their non-bonded distances being in the range of 2.77–3.22 Å (Table 3). In contrast, the corresponding cavity of the 16-membered crown thioether in **6** may be too large compared to the stereochemical size of the hydrido and chloro ligands, and fails to discriminate between these ligands allowing two geometrical isomers **6a** and **6b** to exist both in solution and in the solid state. The coordination of the Cl atom at the congested axial site in the RuCl(*syn*-Me₄[14]aneS₄) moiety of **7** is rather surprising in view of the specific occupation of the hydrido ligand at the stereochemically cluttered axial site in **4**. The direction of the Ru atom displacement from the 4S plane in the RuCl(*syn*-Me₄[14]aneS₄) fragment also differs from that of the RuH(*syn*-Me₄[14]aneS₄) moiety; in the former the Ru1 atom shifts towards the congested side by 0.043(2) Å, while in the latter the Ru2 atom shifts towards the opposite uncluttered side by 0.126(2) Å. The magnitude of the deviation of the Ru2 atom is comparable with that of **4** and its direction is the same for both hydrides (*vide supra*). The geometrical features about the Ru atoms in the RuCl(*syn*-Me₄[14]aneS₄) in **7** and

TABLE 4. Selected bond distances (Å) and angles (°) of {Ru₂H(μ-H)Cl(*syn*-Me₄[14]aneS₄)₂}Cl (**7**)

RuH(<i>syn</i> -Me ₄ [14]aneS ₄) moiety				RuCl(<i>syn</i> -Me ₄ [14]aneS ₄) moiety			
Ru1···Ru2	3.410(2)	Ru1–H _b –Ru2	180	Ru1–Cl	2.589(4)	Cl–Ru1–H _b	180
Ru2–H _t	1.69(13)	H _t –Ru2–H _b	180	Ru1–H _b	1.82(15)	Cl–Ru1–S1(1)	90.6(1)
Ru2–H _b	1.60(15)	H _t –Ru2–S2(1)	85.9(1)	Ru1–S1(1)	2.291(3)	Cl–Ru1–S1(4)	91.6(1)
Ru2–S2(1)	2.299(3)	H _t –Ru2–S2(4)	87.8(1)	Ru1–S1(4)	2.293(3)	H _b –Ru1–S1(1)	89.4(1)
Ru2–S2(4)	2.299(3)	H _b –Ru2–S2(1)	94.1(1)	S1(1)–Cl(2)	1.814(15)	H _b –Ru–S1(4)	88.4(1)
S2(1)–C2(2)	1.827(15)	H _b –Ru2–S2(4)	92.2(1)	S1(4)–Cl(3)	1.806(15)	S1(1)–Ru1–S1(4)	87.7(1)
S2(4)–C2(3)	1.791(15)	S2(1)–Ru2–S2(4)	87.4(1)	S1(4)–Cl(5)	1.844(16)	S1(1)–Ru1–S1(4')	92.3(1)
S2(4)–C2(5)	1.835(13)	S2(1)–Ru2–S2(4')	92.3(1)			S1(1)–Ru1–S1(1')	178.8(2)
		S2(1)–Ru2–S2(1')	171.7(1)			S1(4)–Ru1–S1(4')	176.9(2)
		S2(4)–Ru2–S2(4')	175.7(2)				
Intramolecular non-bonded contacts							
H _t ···H(C2(2))	3.02			Cl···H(Cl(2))	3.23		
H _t ···H(C2(5))	2.51			Cl···H(Cl(5))	2.74		
H _t ···H(C2(7))	2.45			Cl···H(Cl(7))	2.61		

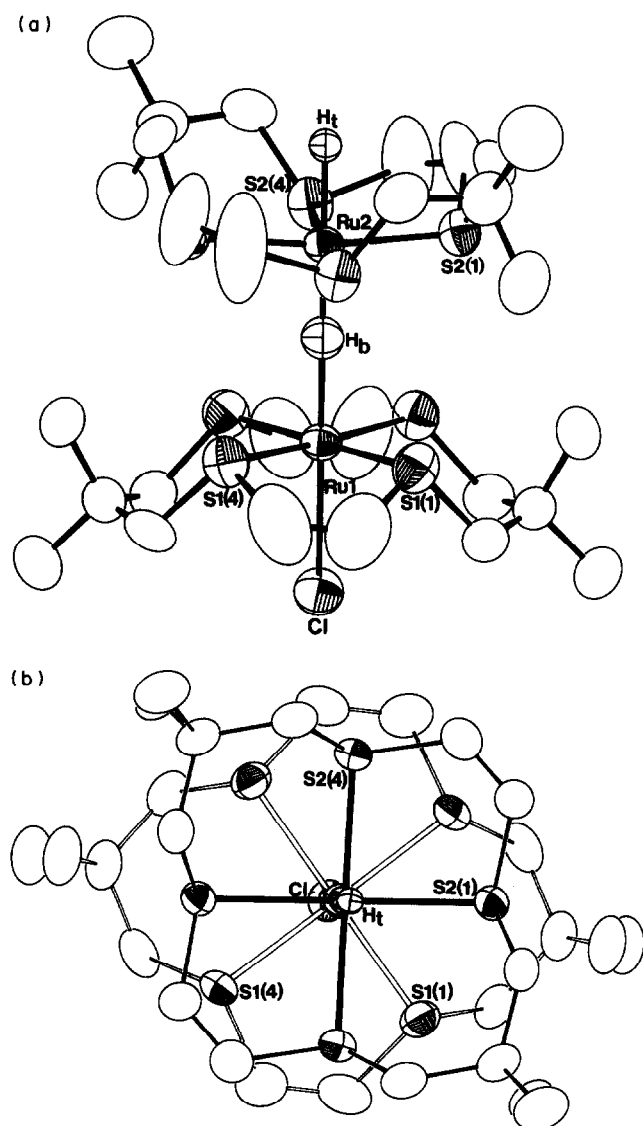
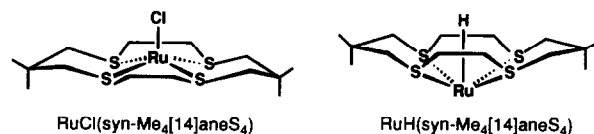


Fig. 5. Molecular structure of the cation of $\{\text{Ru}_2\text{H}(\mu\text{-H})\text{Cl}\}(\text{syn-Me}_4[14]\text{aneS}_4)_2\text{Cl}$ (7) showing a side view (a) and a top view along the C_2 axis (b). Thermal ellipsoids are drawn at 50% probability.

$\text{RuH}(\text{syn-Me}_4[14]\text{aneS}_4)$ moieties in 4 and 7 may be rationalized in terms of the different steric requirements of the two anionic ligands. The spatial volume surrounded by the ring C atoms of $\text{syn-Me}_4[14]\text{aneS}_4$ in 4 proved to have the exact size to accommodate the hydrido ligand. The non-bonded distances between the hydrido ligand and axial CH_2 hydrogen atoms of the $\text{RuH}(\text{syn-Me}_4[14]\text{aneS}_4)$ moiety in 7 ($\text{H} \cdots \text{H}(\text{C}2(5))$ 2.51 and $\text{H} \cdots \text{H}(\text{C}2(7))$ 2.45 Å) are also comparable with those found in 4. Therefore, to admit the more bulky Cl ligand into the congested axial site of Ru ($\text{syn-Me}_4[14]\text{aneS}_4$) moiety, the room should be dilated by bending down the S–C vectors towards the equatorial plane. Such deformation of the $\text{syn-Me}_4[14]\text{aneS}_4$

would displace the Ru atom from the 4S plane towards the congested side along the C_2 axis as shown schematically below. By contrast, an upright deformation of the C–S vectors would induce the deviation towards the opposite uncongested side, which is the case observed for the $\text{RuH}(\text{syn-Me}_4[14]\text{aneS}_4)$ moiety in 4 and 7. Indeed, the crown thioether in the $\text{RuCl}(\text{syn-Me}_4[14]\text{aneS}_4)$ moiety is flattened as shown by the acute dihedral angle [47.4(6°)] between the 4S plane and the least-squares plane defined by the S1(1), S1(4), C1(5), and C1(7) atoms of the $\text{RuSCH}_2\text{CMe}_2\text{CH}_2\text{S}$ ring compared to the corresponding angles of the $\text{RuH}(\text{syn-Me}_4[14]\text{aneS}_4)$ moiety in 4 and 7 (52.5(2) (average) and 53.9(5)°, respectively). Such a displacement of the Ru atom towards the congested axial site may reduce the steric repulsion between the Cl ligand and axial CH_2 hydrogen atoms.



Despite the dilation of the cavity and the displacement of the Ru atom towards the Cl atom, the non-bonded distances between the Cl and axial CH_2 hydrogen atoms at C1(5) and C1(7) (2.74 and 2.61 Å, respectively) are still significantly shorter than the sum of the corresponding van der Waals radii. To avoid the stereochemical repulsions between these atoms as much as possible, the Ru1–Cl bond (2.589(4) Å) is elongated compared to that of 4 (2.559(2) Å) and *trans*- $\text{RuH}(\text{Cl}_2)(\text{diop})_2$ (2.549(1) Å) [23]. The deviation of the Ru atom in 5 from the 4S plane towards the congested axial site can also be explained similarly. The Ru–Cl distance (2.618(2) Å) is again longer than that of 4.

2.4. Linear Ru–H–Ru linkage in $\{\text{Ru}_2\text{H}(\mu\text{-H})\text{Cl}\}(\text{syn-Me}_4[14]\text{aneS}_4)_2\text{Cl}$ (7)

In view of the crystallographic C_2 symmetry of 7, the Ru–H–Ru bond is expected to be linear. The single and unsupported M–H–M bond of transition metals, however, is known to be inherently bent [6,10,11] and this is also the case observed for a Cr–H–Cr linkage in $[\text{Cr}_2(\mu\text{-H})(\text{CO})_{10}]^-$ possessing a D_{4h} non-hydrido framework $[\text{Cr}_2(\text{CO})_{10}]$ [24]. Coupled with the intrinsic limitations of the X-ray diffraction method to determine an accurate hydrido position of heavy transition metal complexes [25], the poor quality of the bond parameters of the H_b ligand in 7 prevents us from delineating the geometry of the Ru–H–Ru bond explicitly. The root mean square amplitude of thermal displacement of the H_b atom normal to the $\text{Ru} \cdots \text{Ru}$ vector is 0.2(3) Å. However, it is worth reminding

ourselves here that the H_b ligand is completely surrounded by the tightly interlocked free lone pair orbitals on the S atoms of the RuH(*syn*-Me₄[14]aneS₄) and RuCl(*syn*-Me₄[14]aneS₄) moieties in a staggered conformation. Should the Ru–H–Ru bond bend and/or rotate, a severe electrostatic repulsion between the S free lone pair electrons of the above two moieties would be expected. To estimate this effect on the geometry of the Ru–H–Ru linkage and on the conformation of the 4S equatorial planes of the two moieties, extended Hückel MO calculations were carried out on a hypothetical model compound {Ru₂H(μ-H)Cl[*syn*-(SH₂)₄]₂}⁺ of C_{4v} symmetry. A Walsch diagram and the total energy as a function of the Ru–H–Ru angle (φ) is shown in Fig. 6. Apparently, the total energy increases sharply on bending the Ru–H–Ru linkage in the symmetry plane from linearity. The molecular or-

bitals relevant to the Ru–H–Ru bond in C_{4v} symmetry are a bonding 1a₁ and a non-bonding 2a₁ consisting mainly of Ru d_{z2} and S p atomic orbitals with H_b s and S s orbitals mixing in for 1a₁ and 2a₁, respectively. These orbitals are relatively low-lying and fully occupied. The increment in total energy assessed on deformation from C_{4v} to C_s symmetry is principally ascribed to the elevation of the 2a₁ orbitals (2a' in C_s) in energy. The destabilization arises from an increase in anti-bonding interactions between d_{z3} orbitals of the Ru atoms and between the free lone pair orbitals on the S atoms of the RuH[*syn*-(SH₂)₄] and RuCl[*syn*-(SH₂)₄] moieties. The Ru···Ru overlap populations calculated for 2a₁ and 2a' at φ = 160° are -0.002 and -0.009, respectively, while the corresponding values between the S atom of one moiety and the nearest two S atoms of the other moiety are -0.004 at φ = 180°

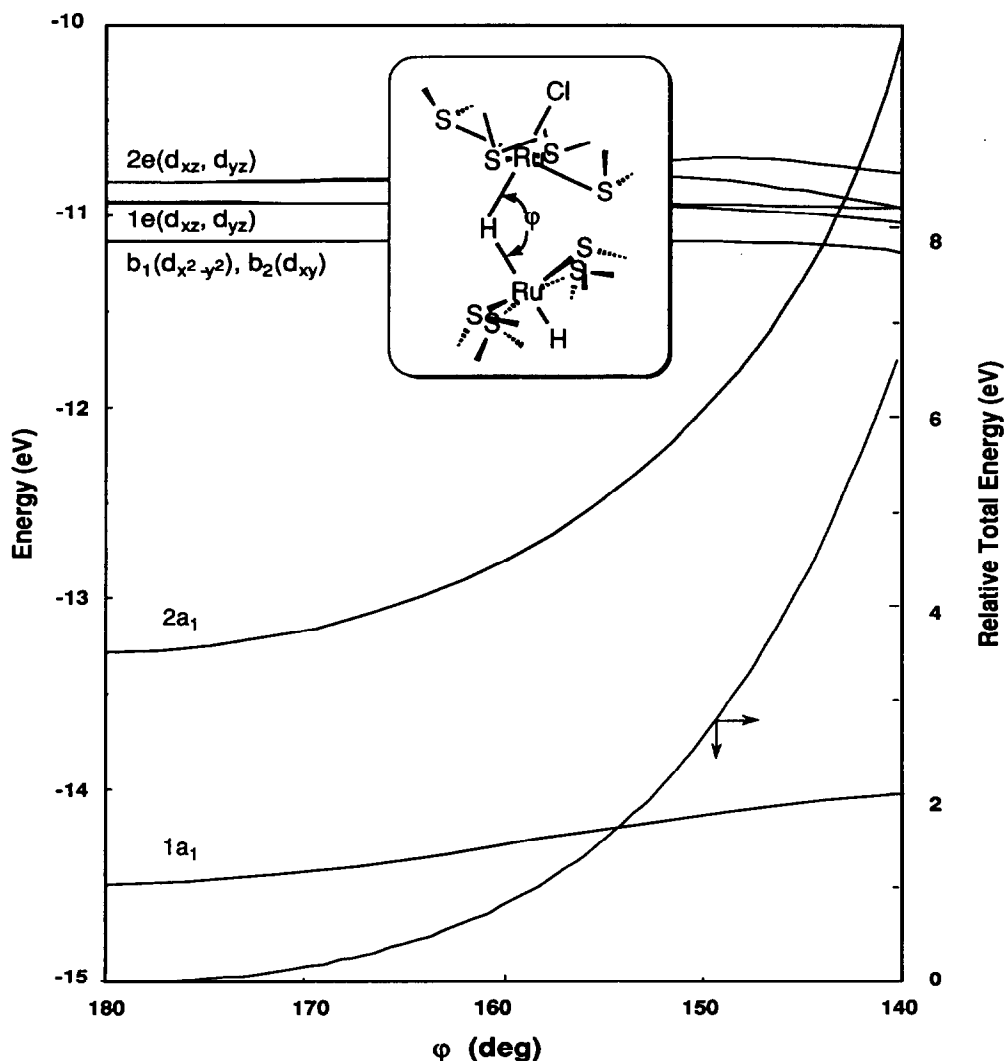


Fig. 6. A Walsch diagram and total energy of {Ru₂H(μ-H)Cl[*syn*-(SH₂)₄]₂}⁺ as a function of the Ru–H–Ru angle (φ).

and -0.146 at 160° . Thus, the antibonding interaction between the lone pair orbitals on S atoms induced on bending plays a principal role in favoring the linear geometry of the Ru–H–Ru linkage. The destabilization in total energy assessed on bending from linearity by 20° is 0.78 eV (Fig. 6).

All the structural and spectral evidence for the single unsupported μ -hydrido bonds of transition metals so far studied support the bent geometry and Bau *et al.* have suggested a 'closed' M–H–M $3c-2e$ bond to represent such bonding, where metal–metal bonding interaction is appreciable and the non-bonding molecular orbital relevant to the M–H–M bond is unoccupied [11].



In accord with a long Ru1...Ru2 separation ($3.410(2)$ Å), the total overlap population between two Ru atoms (0.012) for a linear Ru–H–Ru geometry is negligibly small and this is also the case for the bent one (0.009) with $\varphi = 160^\circ$ where the Ru...Ru distance is assessed to be 3.35 Å. The geometrical deformation of the Ru–H–Ru linkage again does not affect the Ru–H_b bond strengths. Thus, the overlap populations for the H_b–RuCl[*syn*-(SH₂)₄] and H_b–RuH[*syn*-(SH₂)₄] bonds in C_{4v} symmetry are 0.326 and 0.285, respectively and the bond orders remain constant for the bent C_s geometry, the respective populations at $\varphi = 160^\circ$ being 0.326 and 0.285. Thus, the preferred linear geometry of the Ru–H–Ru linkage predicted for

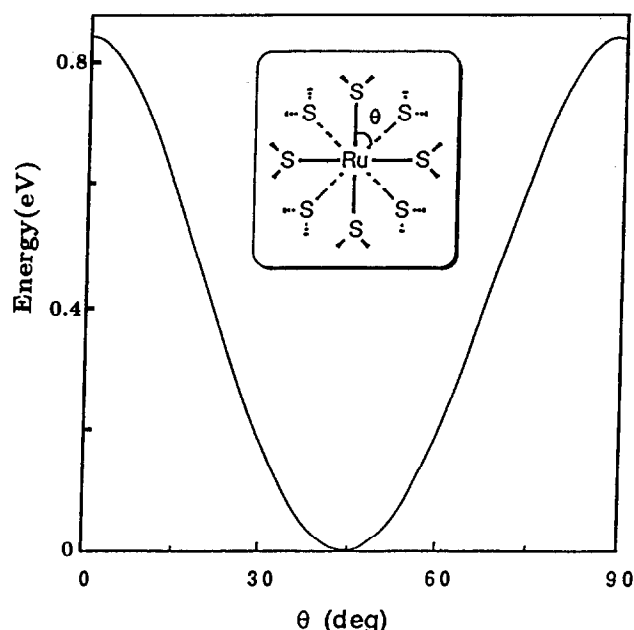
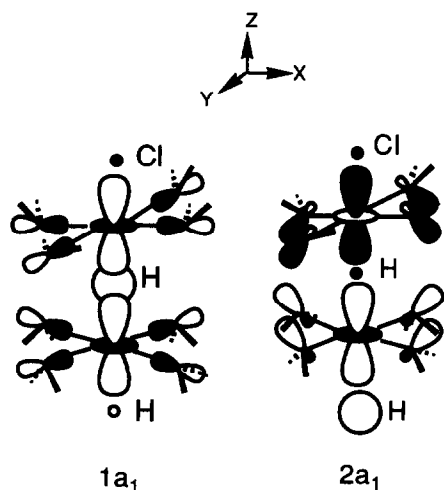


Fig. 7. Variation in the total energy of $\{\text{Ru}_2\text{H}(\mu\text{-H})\text{Cl}\}[\text{syn}-(\text{SH}_2)_4]_2\}^+$ on rotation about the Ru–H–Ru linkage.

7 is ascribed to the filled $2a_1$ orbital which gains antibonding character on bending. On the basis of the theoretical study, the S free lone pair orbitals of the RuH(*syn*-Me₄[14]aneS₄) and RuCl(*syn*-Me₄[14]aneS₄) moieties in the staggered conformation is proved to be crucial in determining the linear Ru–H–Ru geometry. These lone pair orbitals also restrict the rotation about the Ru–H–Ru linkage. Indeed, the variations in total energy assessed for the above model on rotation (Fig. 7) reveal that the staggered conformation is 0.82 eV more stable than the eclipsed one, which agrees with the elucidated structure of 7.

Finally it is worth noting that the single and unsupported Ru–H–Ru bond in 7 is stable even in solution as shown by the strong spin-spin coupling between the terminal and bridging hydrides. The possibility for an interconversion between 4 and 7 by changing the solvent from EtOH to MeOH is also readily excluded since the addition of NaBPh₄ to the MeOH solution of the latter gave exclusively the corresponding salt rather than 8.

3. Concluding remarks

We have clarified two characteristics of the quadridentate crown thioethers adopting a *syn* conformation which affect the discrimination of anionic ligands at the stereochemically different axial sites and the geometry of the Ru–H–Ru linkage in the Ru^{II} hydrido complexes. On the basis of the structural studies of

4–7, the very different congestion at the axial sites of the Ru(*syn*-L) fragment (L = Me₄[14]aneS₄, Me₆[15]aneS₄, Me₈[16]aneS₄) was proved to be capable of discriminating between the hydrido and chloro ligands of different steric requirements. The origin for recognition is simply attractive van der Waals interactions between the CH₂ axial hydrogen atoms of the macrocycles and the anionic ligand coordinated at the congested axial site. The hole size surrounded by the ring carbon atoms is adjustable by the ring size of the macrocycles. Another important conclusion drawn from the observed geometries of the RuX(*syn*-Me₄[14]aneS₄) moiety (X = H, Cl) in 4 and 7 is a flexibility of the *syn*-crown thioether capable of tuning the hole size depending upon the steric bulkiness of an axial ligand to be accommodated. Such a deformation of the crown thioether ligand can induce the geometrical change about the Ru atom, which may also be expected to modify the electronic property of the metal. Coupled with the complete discrimination of the C=O and C=N bonds of PhNCO in *trans*-Mo(η²-O,C-PhNCO)(η²-C,N-PhNCO)(*syn*-Me₄[16]aneS₄) [9], the above results seem to promise that quadridentate crown thioether complexes adopting a *syn* conformation can recognize a wide variety of anionic and π-acidic ligands possessing different steric demands on the axial coordination. The coordinated crown thioethers still exhibit free lone pair orbitals. Their effect on the geometry of the Ru–H–Ru linkage and the conformation of the RuH(*syn*-Me₄[14]aneS₄) and RuCl(*syn*-Me₄[14]aneS₄) moieties in 7 are elucidated theoretically on the basis of the molecular structure. The tight interlocking of the S lone pair orbitals of the two moieties was shown to be crucial for preventing the bending of and the rotation about the Ru–H–Ru bond. The theoretical calculations and the crystallographic C₂ symmetry, thus, strongly suggest that 7 represents the first example of dinuclear μ-hydrido complexes with a linear M–H–M linkage.

4. Experimental details

All manipulations were carried out under a dinitrogen atmosphere. Me₄[14]aneS₄ [26], Me₆[15]aneS₄ [27], RuCl(PPh₃)₃ [28] and RuH(Cl₂)(PPh₃)₃ [29] were prepared according to known procedures. ¹H NMR and IR spectra were recorded on Jeol GX270 and Jasco IR A-100 spectrometers, respectively.

4.1. Preparation of Me₆[15]aneS₄

To disodium ethanedithiolate (13.8 g, 0.1 mol) in EtOH (150 ml) was added 2,2-dimethyl-3-bromopropanol (33.4 g, 0.2 mol) at room temperature and the mixture was heated under reflux for 12 h. The concen-

trated reaction mixture was extracted with CH₂Cl₂ and the concentrated extract was distilled to give 2,2,9,9-tetramethyl-4,7-dithiadecane-1,10-diol (18.5 g, 69%) as a colorless oil (b.p. 170°C/10⁻³ mmHg). ¹H NMR (CDCl₃): δ 0.97 (s, 3H, Me); 2.58 (s, 1H, CH₂); 2.75 (s, 1H, CH₂); 3.43 (s, 1H, CH₂).

To an ice-cooled solution of the diol (18.5 g, 0.069 mol) in pyridine (300 ml) methanesulphonyl chloride (13.0 g, 0.14 mol) was added and the mixture was stirred at 0–5°C for 10 h. After addition of ice-water (850 ml), the mixture was extracted with CHCl₃, washed with dilute HCl and H₂O successively, dried with CaCl₂, and concentrated to give a brown oil.

The crude 2,2,9,9-tetramethyl-4,7-dithiadecane-1,10-bis(methylsulphonate) (25.9 g, 0.13 mol) thus obtained in DMF (200 ml) and disodium 2,2-dimethyl-1,3-dithiolate (11.9 g, 0.66 mol) in DMF (200 ml) were added by the high dilution method to DMF (1800 ml) at 60–70°C for 24 h and the mixture was heated at the same temperature range with stirring for an additional 48 h. The concentrated mixture was extracted with CH₂Cl₂ and washed with H₂O. Chromatography (silica gel, eluant hexane/benzene, 9:1) and subsequent recrystallization of the concentrated residue from pentane/MeOH gave the crown thioether (14.1 g, 58.2%) as colorless crystals, m.p. 72–74°C. Anal. Found: C, 55.28; H, 9.12. C₁₇H₃₄S₄ calcd.: C, 55.74; H, 9.29%. ¹H NMR (CDCl₃): δ 1.02 (s, 6H, Me); 1.06 (s, 3H, Me); 2.25 (s, 2H, CH₂); 2.64 (s, 2H, CH₂); 2.67 (s, 2H, CH₂); 2.84 (s, 2H, CH₂).

4.2. Preparation of *cis*-RuCl₂L (1, L = Me₄[14]aneS₄; 2, L = Me₆[15]aneS₄; 3, L = Me₈[16]aneS₄)

A mixture of RuCl₂(PPh₃)₃ (2.87 g, 3.00 mmol) and Me₄[14]aneS₄ (0.97 g, 3.00 mmol) in toluene (40 ml) was heated at 80°C for 20 h. The pale yellow microcrystals which separated (1.46 g, 98%) were filtered and washed with ether or hexane. The crystals were pure enough to use as a starting material, but may be recrystallized from CH₂Cl₂/toluene; m.p. 277–280°C (dec). Anal. Found: C, 34.52; H, 5.59. C₁₄H₂₈S₄Cl₂Ru calcd.: C, 33.87; H, 5.69%. The compounds 2 and 3 were also obtained by a similar reaction of RuCl(PPh₃)₃ with Me₆[15]aneS₄ and Me₈[16]aneS₄ as yellow (98%) and orange crystals (95%), respectively. Compound 2: m.p. 253–258°C (dec). Anal. Found: C, 38.11; H, 6.29. C₁₇H₃₄S₄Cl₂Ru calcd.: C, 37.91; H, 6.36%. Compound 3: m.p. 265–270°C (dec). Anal. Found: C, 41.60; H, 6.96%. C₂₀H₄₀Cl₂S₄Ru calcd.: C, 41.74; H, 6.96%.

4.3. Preparation of *trans*-RuH(Cl)(*syn*-Me₄[14]aneS₄) (4) and {Ru₂H(μ-H)Cl(*syn*-Me₄[14]aneS₄)₂}Cl (7)

A mixture of *cis*-RuCl₂(Me₄[14]aneS₄) (100 mg, 0.2 mmol) and NaBH₄ (70 mg, 1.85 mmol) in EtOH (10

ml) was stirred at room temperature for 10 h. The orange brown solution was concentrated and the residue was recrystallized from CH₂Cl₂/toluene to give **4** as yellow crystals (15 mg, 16%), m.p. 221–223°C (dec). Anal. Found: C, 36.49; H, 6.06. C₁₄H₂₉ClS₄Ru calcd.: C, 36.40; H, 6.33%. Concentration of the mother liquor and subsequent recrystallization of the solid residue from acetone afforded **7** as brown crystals (50 mg, 54%), m.p. 257–259°C (dec). Anal. Found: C, 36.49; H, 6.13. C₂₈H₅₈Cl₂S₈Ru₂ · 1/2(CH₃)₂CO · H₂O calcd.: C, 36.53; H, 6.44%. Addition of NaBPh₄ to a MeOH solution of **7** and recrystallization of the precipitates from acetone gave the corresponding BPh₄ salt quantitatively. Anal. Found: C, 53.06; H, 6.68. C₅₂H₆₂BClS₈Ru₂ · Me₂CO calcd.: C, 52.62; H, 6.85%.

Compound **4** can be prepared in high yield (81%) by carrying out the above reaction under similar conditions but in MeOH.

4.4. Preparation of *trans*-RuH(Cl)L (**5**, L = *syn*-Me₆[15]aneS₄; **6**, L = *syn*-Me₈[16]aneS₄)

cis-RuCl₂(Me₆[15]aneS₄) (200 mg, 0.37 mmol) was treated with NaBH₄ (14 mg, 0.37 mmol) in EtOH (40 ml) at room temperature for 3 h. After concentration of the yellow solution *in vacuo*, the residue was extracted with toluene and recrystallized by adding hexane to the concentrated solution to give **5** as yellow crystals in 50% yield, m.p. 195–200°C (dec). Anal. Found: C, 40.91; H, 6.90. C₁₇H₃₅ClS₄Ru calcd.: C, 40.50; H, 6.99%.

A similar reaction of *cis*-RuCl₂(Me₈[16]aneS₄) with an equimolar amount of NaBH₄ gave **6** as yellow

crystals in 74% yield, m.p. 250°C (dec). Anal. Found: C, 44.09; H, 7.39. C₂₀H₄₁ClS₄Ru calcd.: C, 43.99; H, 7.57%.

4.5. Preparation of {RuH(*syn*-Me₄[14]aneS₄)}BPh₄ (**8**)

To a solution of *trans*-RuH(Cl)(*syn*-Me₄[14]aneS₄) (30 mg, 0.065 mmol) in EtOH was added an excess of NaBPh₄ at room temperature and the resulting precipitate was recrystallized from acetone to give **8** as pale yellow crystals (26 mg, 54%). Anal. Found: C, 61.26; H, 6.48. C₃₈H₄₉BS₄Ru calcd.: C, 61.20; H, 6.62%.

4.6. Preparation of RuH(Cl)(PPh₃)₂(Me₄[14]aneS₄) (**9**)

To a suspension of RuH(Cl)(PPh₃)₃PhCH₃ (146 mg, 0.14 mmol) in DME (15 ml) was added Me₄[14]aneS₄ at room temperature. After several minutes, the purple crystals of the starting material dissolved to give a reddish brown solution. Concentration of the filtered solution gave yellow crystals of **9** (127 mg, 85%), m.p. 105–107°C (dec). Anal. Found: C, 60.20; H, 6.25. C₅₀H₅₉ClP₂S₄Ru · MeOCH₂CH₂OMe calcd.: C, 60.24; H, 6.96%. An attempt to prepare the Me₈[16]aneS₄ analogue failed; even under prolonged heating (60°C, 44 h) of RuH(Cl)(PPh₃)₃ with the crown thioether in DME, the starting materials were recovered unchanged.

4.7. Preparation of {RuH(PPh₃)(Me₄[14]aneS₄)}BPh₄ (**10**)

The compound **9** (53 mg, 0.05 mmol) was dissolved in MeOH (10 ml) and an excess of NaBPh₄ was added to precipitate **10** quantitatively. Recrystallization from CH₂Cl₂/MeOH gave pale yellow crystals, m.p. 223–

TABLE 5. Crystallographic data for diffraction studies

Compound	4	5	7
Formula	C ₁₄ H ₂₉ ClS ₄ Ru	C ₁₇ H ₃₅ ClS ₄ Ru	C ₂₈ H ₅₈ Cl ₂ S ₈ Ru ₂ · 1/2Me ₂ CO · H ₂ O
F.W.	462.2	504.2	971.2
Crystal system	Orthorhombic	Orthorhombic	Trigonal
<i>a</i> (Å)	14.683(13)	14.976(3)	18.615(6)
<i>b</i> (Å)	12.605(2)	13.877(3)	
<i>c</i> (Å)	10.284(7)	21.087(27)	64.937(13)
<i>V</i> (Å ³)	1903(2)	4381(6)	19487(11)
<i>Z</i>	4	8	18
<i>d</i> _{calc} (g cm ⁻³)	1.61	1.52	1.49
Space group	<i>Pna</i> 2 ₁	<i>Pbca</i>	<i>R</i> $\bar{3}c$
Crystal size (mm)	0.5 × 0.5 × 0.5	0.4 × 0.4 × 0.3	0.3 × 0.3 × 0.2
μ (cm ⁻¹)	15.80	7.78	17.3
Scan type	2 θ - ω	2 θ - ω	2 θ - ω
2 θ range (°)	3–60	3–55	5–55
No. data collected	3167	5064	5204
No. of unique data	2303 ($ F_o > 6\sigma(F_o)$)	3011 ($ F_o > 5\sigma(F_o)$)	1975 ($ F_o > 6\sigma(F_o)$)
No. of parameters	186	213	225
<i>R</i> (<i>R</i> _w)	0.030(0.033)	0.043(0.051)	0.055(0.063)
GOF	1.29	1.28	1.42

225°C (dec). Anal. Found: C, 66.39; H, 6.39. C₅₆H₆₄BPS₄-Ru calcd.: C, 66.72; H, 6.40%.

4.8. X-Ray structural studies of *trans*-RuH(Cl)(*syn*-L) (4, L = Me₄[14]aneS₄; 5, L = Me₆[15]aneS₄) and {Ru₂H(μ-H)Cl(Me₄[14]aneS₄)₂}Cl · 1/2Me₂CO · H₂O (7)

4.8.1. Data collection

Air sensitive crystal of 4, 5 and 7 suitable for X-ray diffraction experiments were grown from CH₂Cl₂/toluene, EtOH, and acetone, respectively. Intensities were collected on a Rigaku AFC-6 automatic four-circle diffractometer by using graphite-monochromated Mo-Kα radiation (μ = 0.71068 Å). Unit cell parameters of 4, 5 and 7 were obtained from least-squares refinements of 24 (38 ≤ 2θ ≤ 40°), 20 (22 ≤ 2θ ≤ 26°), and 20

reflections (26 ≤ 2θ ≤ 32°) measured at room temperature, respectively. The refined cell parameters and additional relevant crystal data are summarized in Table 5. The intensities of three reflections were monitored every 100 reflections; no significant decay (< 2%) was observed during the data collections for these complexes. The data were corrected for *Lp* effect, but not for absorption (μ_r = 0.4, 0.16, and 0.3 for 4, 5 and 7, respectively).

4.8.2. Structural solution for 4 and 5

All calculations were performed on an ACOS-930 computer using UNICS II [30]. The positions of the Ru atoms were located from Patterson maps. The systematic absences for the reflections limited the choice of space groups to *Pna*2₁ or *Pnam* for 4 and *Pbca* for 5.

TABLE 6. Selected atomic coordinates (×10⁴) and isotropic thermal parameters (Å² × 10³) for 4, 5 and 7

Atom	x	y	z	U _{eq}	Atom	x	y	z	U _{eq}
<i>trans</i> -RuH(Cl)(<i>syn</i> -Me ₄ [14]aneS ₄) (4)									
Ru	6436.6(2)	4769.8(3)	0.6(1)	29.1(1)	C(9)	8383(4)	5461(5)	-1295(7)	49(3)
Cl	695(1)	4543(1)	2390(1)	45(1)	C(10)	8110(4)	4427(5)	-1893(6)	50(3)
S(1)	5321(1)	3530(1)	267(1)	35(1)	C(12)	6990(4)	2669(4)	-1867(5)	45(3)
S(4)	5363(1)	6036(1)	527(1)	40(1)	C(13)	6199(4)	1997(4)	-1332(6)	47(3)
S(8)	7465(1)	6111(1)	-415(1)	36(1)	C(14)	5322(3)	2629(4)	-1119(5)	39(3)
S(11)	7509(1)	3585(1)	-711(1)	35(1)	C(Me1)	6358(4)	8230(4)	-1(1)	64(3)
C(2)	4314(3)	4283(4)	-197(6)	29(2)	C(Me2)	5841(4)	8265(4)	-2356(7)	58(3)
C(3)	4273(3)	5320(4)	536(6)	37(2)	C(Me3)	6479(4)	1411(4)	-6(1)	64(3)
C(5)	5244(3)	6860(4)	-918(5)	45(3)	C(Me4)	5975(4)	1188(5)	-1399(9)	65(4)
C(6)	6105(4)	7545(4)	-1215(5)	50(3)	H	603(4)	489(5)	-152(8)	47(21)
C(7)	6936(4)	6911(4)	-1688(5)	48(3)					
<i>trans</i> -RuH(Cl)(<i>syn</i> -Me ₆ [15]aneS ₄) (5)									
Ru	3408.9(3)	3504.8(3)	2958.4(2)	27.8(2)	C(10)	5268(4)	2062(4)	2723(3)	34(3)
Cl	4636(1)	4831(1)	2815(1)	41(1)	C(11)	5402(4)	2255(4)	3016(30)	35(3)
S(1)	2802(1)	3616(1)	1962(1)	40(1)	C(13)	4929(4)	2826(5)	1862(3)	40(3)
S(4)	2345(1)	4635(1)	3232(1)	34(1)	C(14)	4332(4)	3037(5)	1292(3)	61(4)
S(8)	3812(1)	3302(1)	4002(1)	37(1)	C(15)	3689(4)	3890(5)	1409(3)	56(3)
S(12)	4373(1)	2348(1)	2561(1)	37(1)	C(Me1)	3325(5)	5879(5)	4830(4)	83(6)
C(2)	2149(5)	4737(5)	1957(3)	66(5)	C(Me2)	2317(4)	4556(6)	4713(3)	46(4)
C(3)	2340(5)	5355(5)	2500(4)	82(5)	C(Me3)	6198(4)	1805(5)	3989(3)	51(4)
C(5)	2849(4)	5516(4)	3760(3)	45(4)	C(Me4)	4634(4)	1222(5)	3831(3)	55(4)
C(6)	3085(4)	5102(5)	4406(3)	46(3)	C(Me5)	3833(5)	2128(5)	1076(3)	83(3)
C(7)	3945(4)	4489(4)	4380(3)	49(4)	C(Me6)	4968(5)	3362(6)	760(3)	86(6)
C(9)	4988(4)	2980(4)	4078(3)	35(3)	H	265(4)	279(5)	311(3)	40(20)
{Ru ₂ H(μ-H)Cl(<i>syn</i> -Me ₄ [14]aneS ₄) ₂ }Cl (7)									
Ru1	0	4692(1)	2500	40(1)	Ru2	0	2860(1)	2500	34(1)
S1(1)	1046(2)	5202(2)	2739.0(5)	61(2)	S2(1)	-172(2)	2684(2)	2850.5(4)	52(2)
S1(4)	1004(2)	5160(2)	2250.0(5)	48(2)	S2(4)	-1421(2)	2103(2)	2472.4(5)	43(2)
Cl(2)	1865(9)	6020(10)	2588(3)	60(10)	C2(2)	-1203(8)	1760(10)	2866(2)	64(9)
Cl(3)	1880(10)	5970(10)	2386(3)	80(10)	C2(3)	-1710(10)	1650(10)	2723(2)	70(10)
Cl(5)	766(8)	5747(7)	2060(2)	100(10)	C2(5)	-1674(7)	1194(7)	2312(2)	59(8)
Cl(6)	-44(9)	5250(8)	1946(2)	110(10)	C2(6)	-1380(8)	1402(7)	2090(2)	65(8)
Cl(7)	-820(8)	4984(8)	2076(2)	90(10)	C2(7)	-444(8)	1776(7)	2066(2)	85(9)
Cl(Me1)	-7(1)	4515(9)	1836(2)	150(20)	C2(Me1)	-1688(8)	1943(8)	1991(2)	76(9)
Cl(Me2)	-5(1)	5839(9)	1779(2)	150(10)	C2(Me2)	-1765(9)	563(9)	1982(2)	90(10)
H _t	0	1950(70)	2500	30(43)	H _b	0	372(8)	2500	53(51)
Cl	0	6082(1)	2500	78(3)					

Attempts to solve the structure in the centric space group *Pnam* for the former were not successful. All non-hydrogen atoms were found by successive difference Fourier syntheses and were refined by the block-diagonal least-squares method with anisotropic temperature factors. The hydrogen atoms of the macrocycles were included at the calculated positions (C–H = 0.96 Å) with $B_{\text{iso}} = 4.0 \text{ \AA}^2$; their parameters were not refined. The hydrido ligands of both complexes were found in the difference Fourier maps at this stage. In the final least-squares refinements, the positional and temperature factors of the hydrido ligands were carefully refined isotropically. Tables of atomic coordinates and anisotropic thermal factors, bond distances and angles, and observed and calculated structure factors for **4** have been deposited at the Cambridge Crystallographic Data Center [12] while those of **5** are available as supplementary material.

4.8.3. Structural solution of **7**

In the first stage, the analysis was carried out for the small yet false triclinic system (*P1*) to give only an approximate crystal structure possessing pseudo C_3 symmetry ($Z = 6$). The correct crystal system was found to be trigonal with a very long *c*-axis as shown in Table 5. Systematic absences $hk(i)l$ for $-h + k + l \neq 3n$ and $hh(0)l$ for $l = 2n + 1$ were consistent with both $R\bar{3}c$ and $R3c$ space groups. The structure could be solved and refined successfully in the former space group. The positions of two Ru atoms were determined from the Patterson map. Phases derived from the Ru positions were used to locate all S atoms and the Cl ligand. All other non-hydrogen atoms including the Cl counter anion were found by a series of difference Fourier and block diagonal least-squares refinements. The H atoms of H₂O were detected and refined isotropically, while those of the macrocycle and Me₂CO were included at the calculated positions (C–H = 0.96 Å) with $B_{\text{iso}} = 4.0 \text{ \AA}^2$ and their positions were not refined. At this stage, the H_t and H_b atoms were found in difference Fourier maps using the low-angle reflections ($\sin\theta/\lambda < 0.40 \text{ \AA}^{-1}$) and refined isotropically by fixing the positional and thermal parameters of all other atoms [31]. It is to be noted that the difference Fourier synthesis employing the whole reflection data showed promise in locating the hydrido peaks, but they were merged by a number of background peaks. Finally the other atoms were refined by fixing the refined parameters of the hydrido ligands. The abnormal C–C bond lengths of the RuSCH₂CH₂S rings are caused by the large anisotropic thermal motions of the C atoms. The difference Fourier maps did not show any disorder about these C atoms. The final difference Fourier synthesis displayed no significant residual electron density; the

largest peak was 0.50 e \AA^{-3} at (1/3, 1/3, 0.085) on a threefold screw axis. Atom scattering factors and anomalous dispersion terms were taken from common sources. Atomic coordinates and thermal parameters, full bond lengths and angles and $F_o - F_c$ tables are deposited as supplementary materials.

4.9. Molecular orbital calculations

All calculations were of the extended Hückel type with weighted H_{ij} 's. The valence state ionization potentials and orbital exponents of Ru 4d, 5s and 5p orbitals were taken from those given by Hoffmann *et al.* [32]. The parameters for H, S and Cl atoms are standard. Bond lengths and angles for the model compound are those found for **7** except S–H distance of 1.33 Å.

Acknowledgement

This work is partly supported partly by a Grant-in-Aid for Scientific Research (No. 02804050) from the Ministry of Education, Science and Culture, Japan and by Takasago Research Institute, Inc. We thank Professor Kazuyuki Tatsumi of Department of Chemistry, Faculty of Engineering Science, Osaka University for valuable suggestions on the theoretical calculations.

References

- 1 K.S. Suslick and T.J. Reinert, *J. Chem. Educ.*, **62** (1985) 974 and refs. therein.
- 2 D.H. Busch, L.L. Zimmer, J.J. Grzybowski, D.J. Olszauski, S.C. Jackels, R.C. Callahan and G.G. Christoph, *Proc. Natl. Acad. Sci. USA*, **8** (1981) 5951.
- 3 (a) W.-K. Lin, N.W. Alcock and D.H. Busch, *J. Am. Chem. Soc.*, **113** (1991) 7603; (b) D.H. Busch, in A.F. Martell and D.T. Sawyer (eds.), *Oxygen Complexes and Oxygen Activation by Transition Metals*, Plenum, New York, 1988, p. 61.
- 4 (a) J.F. Endicott, J. Kumar, C.L. Schwarz, M.C. Perkovic and W.-K. Lin, *J. Am. Chem. Soc.*, **111** (1989) 7411; (b) C.L. Schwarz and J.F. Endicott, *Inorg. Chem.*, **28** (1989) 4011 and refs. therein.
- 5 T. Yoshida, T. Adachi, K. Kawazu and N. Sasaki, *Angew. Chem., Int. Ed. Engl.*, **30** (1991) 982.
- 6 D.W. Hart, R. Bau and T.F. Koetzle, *Organometallics*, **4** (1985) 1590 and refs. therein.
- 7 J.P. Olsen, T.F. Koetzle, S.W. Kirtley, M. Andrew, D.L. Tipton and R. Bau, *J. Am. Chem. Soc.*, **96** (1974) 6621.
- 8 W.A. Herrmann, H. Biersack, M.L. Ziegler, and P. Wülknitz, *Angew. Chem., Int. Ed. Engl.*, **20** (1981) 388.
- 9 A. Albinatti, R. Naegeli, A. Tongni and L.M. Vananzi, *Organometallics*, **2** (1983) 926.
- 10 F.A. Cotton and G. Wilkinson, *Advanced Inorganic Chemistry*, 5th edition, Wiley, New York, 1988.
- 11 R. Bau, R.G. Teller, S.W. Kirtley and T.F. Koetzle, *Acc. Chem. Res.*, **12** (1979) 176 and refs. therein.
- 12 T. Yoshida, T. Adachi, T. Ueda, T. Tanaka and F. Goto, *J. Chem. Soc. Chem. Commun.*, (1990) 342.
- 13 T. Yoshida, T. Adachi, T. Tanaka and F. Goto, *J. Organomet. Chem.*, **428** (1992) C12.

- 14 T. Ueda, H. Yamanaka, T. Adachi and T. Yoshida, *Chem. Lett.*, (1988) 525.
- 15 A.J. Blake and M. Schröder, *Adv. Inorg. Chem.*, 35 (1990) 1; A.F. Hill, N.W. Alcock, J.C. Cannadine and G.R. Clark, *J. Organomet. Chem.*, 426 (1992) C40; N.W. Alcock, J.C. Cannadine, G.R. Clark and A.F. Hill, *J. Chem. Soc., Dalton Trans.*, (1993) 1131.
- 16 T.-F. Lai and C.-K. Poon, *J. Chem. Soc., Dalton Trans.*, (1982) 1465.
- 17 T. Yoshida, T. Adachi, H. Akao and T. Tanaka, unpublished.
- 18 T.H. Tulip, T. Yamagata, T. Yoshida, R.D. Wilson, J.A. Ibers and S. Otsuka, *Inorg. Chem.*, 18 (1979) 2239.
- 19 K. Osakada, K. Ohshiro and A. Yamamoto, *Organometallics*, 10 (1991) 404.
- 20 S.C. Rawle, T.J. Sewell and S.R. Cooper, *Inorg. Chem.*, 26 (1987) 33769.
- 21 S.C. Rawle and S.R. Cooper, *J. Chem. Soc., Chem. Commun.*, (1987) 308.
- 22 M.N. Bell, A.J. Blake, M. Schröder, H.-J. Küppers and K. Wieghardt, *Angew. Chem., Int. Ed. Engl.*, 26 (1987) 250.
- 23 R.G. Ball and J. Trotter, *Inorg. Chem.*, 20 (1981) 261.
- 24 J. Roziere, J.M. Williams, R.P. Jr. Stewart, J.L. Petersen and L.F. Dahl, *J. Am. Chem. Soc.*, 99 (1977) 4497.
- 25 R. Bau, R.G. Teller, S.R. Kirtley and T.F. Koetle, *Acc. Chem. Res.*, 12 (1979) 176.
- 26 E.R. Wolf and S.R. Cooper, American Chemical Society, Seattle, 1989, abstract INORG 173.
- 27 T. Yoshida, T. Adachi, T. Ueda, M. Watanabe, M. Kaminaka and T. Higuchi, *Angew. Chem., Int. Ed. Engl.*, 26 (1987) 1171.
- 28 P.S. Hallmann, T.A. Stephenson and G. Wilkinson, *Inorg. Synth.*, 12 (1970) 237.
- 29 R.A. Schunn and E.R. Wonchoba, *Inorg. Synth.*, 13 (1972) 131.
- 30 T. Ashida, *The Universal Crystallographic Computing System-Osaka*, The Computer Center, Osaka University, 1979.
- 31 S.L. Palca and J.A. Ibers, *Acta Crystallogr.*, 18 (1965) 511; S.W. Kirtley, J.P. Olsen and R. Bau, *J. Am. Chem. Soc.*, 95 (1973) 4532.
- 32 K. Tatsumi and R. Hoffmann, *J. Am. Chem. Soc.*, 103 (1981) 328.